A Novel Parameter Determination Method for Lq Regularization Based Sparse SAR Imaging

Jia-cheng Ni[1(✉)], Qun Zhang[1,2], Li Sun[1], and Xian-jiao Liang[3]

[1] Information and Navigation College, Air Force Engineering University, Xi'an 710077, China
littlenjc@sina.com
[2] Collaborative Innovation Center of Information Sensing and Understanding, Xi'an 710077, China
[3] Unit 95100 of PLA, Guangzhou 510405, China

Abstract. Sparse SAR imaging based on Lq($0 < q < 1$) regularization has become a hot issue in SAR imaging. However, it can be difficult to determine a suitable value of the regularization parameter. In this paper, we developed a novel adaptive regularization parameter determination method for Lq regularization based SAR imaging. On the basis that the noise type in SAR system is mostly additive Gaussian white noise, we present a method for determining the regularization parameter through evaluating the statistics of noise. The parameter is updated through validating the statistical properties of the reconstruction error residuals in a suitable Noise Confidence Region (NCR). The experiment results illustrate the validity of the proposed method.

Keywords: SAR imaging · Lq($0 < q < 1$) regularization
Regularization parameter determination

1 Introduction

SAR imaging can be seen as an ill-posed inverse scattering problem whereby a spatial map of reflectivity is reconstructed from measurements of scattered fields [1]. In conventional SAR imaging, the data must be acquired at the Nyquist rate. The recently emerging of compressed sensing (CS) suggests that it is possible to recover a sparse signal from only a small number of random measurements, which permits signals to be sampled at the sub-Nyquist rate. More recently, another type of reconstruction algorithms called Lq norm regularization, have been utilized for radar imaging. Specially, when $q \leq 1$, many advantages over conventional radar imaging were demonstrated including enhanced features, increased resolution and reduced sidelobes. The L1 regularization is used in radar imaging in [2] as an alternative method for L0 regularization

The authors would like to express thanks for the support of the Aeronautical Science Foundation (Grant No. 20151996016) and Coordinate Innovative Engineering Project of Shaanxi Province (Grant No. 2015KTTSGY0406).

X. Gu et al. (Eds.): MLICOM 2017, Part II, LNICST 227, pp. 150–159, 2018.
https://doi.org/10.1007/978-3-319-73447-7_18

in CS [3, 4]. Since L1 regularization is a convex problem, it can be very efficiently solved. In [5], Lq $(0<q<1)$ regularization was introduced as a further improvement upon L1 regularization, it proves that Lq $(0<q<1)$ regularization can assuredly generate much sparser solutions than L1 regularization. Because of this, the Lq $(0<q<1)$ regularization has been accepted as a useful tool for solving the sparse SAR imaging problems.

In Lq regularization based SAR imaging approaches, the regularization parameter λ has a substantial impact on the imaging result. Inappropriate choice of these parameters can either trap the algorithm in local minima and/or lead to a lower convergence rate. Specifically, in SAR imaging task, if λ is too small, sidelobes are only partially reduced and there will still exist some noise. If λ is too large, the reconstruction image will be over-smoothed [6]. Usually, λ is set to be a fixed constant (greater than 0). However, the original setting of λ doesn't always apply to all imaging situations. There are also some methods been proposed to iteratively update the regularization parameters, such as use of the discrepancy principle [7] that seeks for the noise-only residual, and L-curve, which is based on the plot of the norm of the regularized solution versus the norm of the corresponding residual [8]. However, this type of methods suffers a time-consuming iterative process and may decreases the convergence of Lq reconstruction algorithms, which seriously limits the wide use of these methods.

In this paper, we present a regularization parameter determination method based on the properties of the additive noise. By assuming that the radar system noise and other additive noise follow the white Gaussian distribution, we define a probabilistic region of confidence for the noise coefficients. We update λ at the end of each iteration so that the statistical properties of the error residuals can fall into the noise confidence region. The updating algorithm stops when the residual has a Gaussian like structure. This method can avoid the over-smoothing without lowering the convergence speed.

The reminder of this paper is organized as follows. Section 2 presents the Sparse SAR imaging approach based on Lq regularization framework. Section 3 presents the regularization parameter determination method. Section 4 shows some simulation results to verify the effectiveness of the proposed approach. Section 5 provides the conclusion.

2 Sparse SAR Imaging Based on Lq Regularization

2.1 SAR Observation Model

The geometry of the SAR imaging system and the observation scene is shown in Fig. 1. Supposing the velocity of the platform is v. The transmitted signal of SAR imaging system is the linear-frequency-modulated (LFM) signals, which can be modeled by

$$s(\hat{t}, t_m) = \mathrm{rect}\left(\frac{\hat{t}}{T_\mathrm{p}}\right) \cdot \exp\left[\mathrm{j}2\pi f_0 t + \mathrm{j}\pi\gamma\hat{t}^2\right] \tag{1}$$

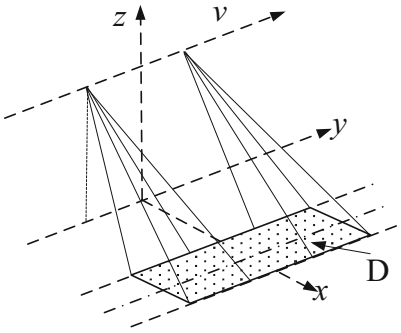

Fig. 1. SAR imaging geometry.

where $\hat{t}$ is the fast time, $t = \hat{t} + t_m$ is the full time, t_m is the slow time; $rect\left(\hat{t}/T_p\right)$ is the rectangular window with a width of T_p, T_p is the pulse repetition interval; f_0 is the carrier frequency and γ is the chirp rate. The received two dimensional SAR data can be written as:

$$s(\hat{t}, t_m) = \iint_D \sigma(x,y) \cdot \text{rect}\left(\frac{\hat{t} - \tau(x,y)}{T_\text{p}}\right) \cdot \exp\left[\text{j}\pi\gamma(\hat{t} - \tau(x,y))^2 - \text{j}2\pi f_0 \tau(x,y)\right] dxdy \tag{2}$$

where D is the imaging area, (x, y) is the coordinates of scatteres in D and $\sigma(x, y)$ denotes the scattering reflectivity coefficient at (x, y). $\tau(x,y) = 2\sqrt{y^2 + (x - u_m)^2}\Big/c$ is the delay of the echo signal, $u_m = v \cdot t_m$ is the platform position and c is the speed of light. Now assume that the imaging scene is discrete into a point-scattering model, which includes $M \times N$ scatterers with the scattering coefficients $\sigma(x, y)$, $x = 1, 2, \ldots, M$ and $y = 1, 2, \ldots, N$. Therefore, (2) can be expressed as:

$$s(\hat{t}, t_m) = \sum_{x=1}^{M}\sum_{y=1}^{N} \sigma(x,y) \cdot \text{rect}\left(\frac{\hat{t} - \tau(x,y)}{T_\text{p}}\right) \cdot \exp\left[\text{j}\pi\gamma(\hat{t} - \tau(x,y))^2 - \text{j}2\pi f_0 \tau(x,y)\right] \tag{3}$$

Due to the sampling process, the radar fast and slow times are also discrete, so (3) can change into expression as:

$$s\left(\hat{t}_p, t_{m,q}\right) = \sum_{x=1}^{M}\sum_{y=1}^{N} \sigma(x,y) \cdot \text{rect}\left(\frac{\hat{t}_p - \tau(x,y)_q}{T_\text{p}}\right) \cdot \exp\left[\text{j}\pi\gamma\left(\hat{t}_p - \tau(x,y)_q\right)^2 - \text{j}2\pi f_0 \tau(x,y)_q\right]$$
$$p = 1, 2, \ldots, P; \qquad q = 1, 2, \ldots, Q; \tag{4}$$

where P is the samples of fast time and Q is the samples of slow time. $\tau(x,y)_q$ is the echo delay of scatterer (x,y) at slow time $t_{m,q}$.

2.2 Lq Regularization Based SAR Imaging

After the data discretization in (4), we put all the scattering coefficients $\sigma(x,y)$ into a column vector and change (4) into a more general matrix form as:

$$s = \mathbf{H}g + n_0 \tag{5}$$

where $s \in \mathbb{C}^{PQ\times 1}$ is the column vector of radar echo, $\mathbf{H} \in \mathbb{C}^{PQ\times MN}$ is the observation matrix, $g \in \mathbb{C}^{MN\times 1}$ is the column vector of scattering coefficients and $n_0 \in \mathbb{C}^{PQ\times 1}$ is the system noise. In (5) we have:

$$\begin{aligned} s &= \left[s(\hat{t}_1, t_{m,1}), \ldots, s(\hat{t}_1, t_{m,Q}), s(\hat{t}_2, t_{m,1}) \ldots, s(\hat{t}_2, t_{m,Q}), \ldots, s(\hat{t}_P, t_{m,1}), \ldots, s(\hat{t}_P, t_{m,Q})\right]^{\mathrm{T}} \\ g &= [\sigma(1,1), \ldots, \sigma(M,1), \ldots, \sigma(1,N), \ldots \sigma(M,N)]^{\mathrm{T}} \end{aligned} \tag{6}$$

The observation matrix $\mathbf{H}$ can be expressed as:

$$\mathbf{H} = \left[h(\hat{t}_1, t_{m,1}), \ldots, h(\hat{t}_1, t_{m,Q}), h(\hat{t}_2, t_{m,1}) \ldots, h(\hat{t}_2, t_{m,Q}), \ldots, h(\hat{t}_P, t_{m,1}), \ldots, h(\hat{t}_P, t_{m,Q})\right]^{\mathrm{T}} \tag{7}$$

where $h(\hat{t}_p, t_{m,q})$ contains the radar phase terms and rectangular window terms in (4), which can be written as:

$$\begin{aligned} h(\hat{t}_p, t_{m,q}) &= \left[h(\hat{t}_p, t_{m,q}, 1), h(\hat{t}_p, t_{m,q}, 2), \ldots, h(\hat{t}_p, t_{m,q}, MN)\right]^{\mathrm{T}} \\ h(\hat{t}_p, t_{m,q}, i) &= \mathrm{rect}\left(\frac{\hat{t}_p - \tau(x,y,i)_q}{T_{\mathrm{p}}}\right) \cdot \exp\left[\mathrm{j}\pi\gamma\left(\hat{t}_p - \tau(x,y,i)_q\right)^2 - \mathrm{j}2\pi f_0 \tau(x,y,i)_q\right] \\ i &= 1, 2, \ldots, MN \end{aligned} \tag{8}$$

From (8) we get the projection relationship between imaging scene g and radar echo s. In CS-based SAR imaging, s is compressed with a sampling matrix $\mathbf{\Theta} \in \mathrm{C}^{r\times PQ}$, $r \ll MN$, so (5) can be change into:

$$s_s = \mathbf{\Theta}\mathbf{H}g + n_s \tag{9}$$

When g is a sparse scene, say, most of the scatters in g are zeros, the theory of CS tells when and how it can be recovered from the above ill-posed linear system. If the sensing matrix $\mathbf{A} = \mathbf{\Theta}\mathbf{H}$ satisfies conditions like RIP [3], g can be exactly recovered using the Lq (quasi-norm) $(0 \le q \le 1)$ regularization optimization:

$$\hat{g} = \underset{g}{\operatorname{argmin}} \left\{ \|\mathrm{s}_s - \mathbf{A}g\|_2^2 + \lambda \|g\|_q^q \right\} \tag{10}$$

where $\lambda > 0$ is the regularization parameter.

The first term in objective function (10) is called a data fitting term, which corresponds to model (9), and represents the observation geometry. The second term is called the regularization term regarding the behavior of the scene g. Regularization parameter λ controls the trade-off between data-fidelity and reconstruction sparsity, which plays a crucial role in the regularization optimization.

3 Regularization Parameter Determination Method

In this section we present a regularization parameter determination method using the statistics of noise. We first introduce the concept of Noise Confidence Region (NCR) and derive the upper boundary and lower boundary of NCR. We then present our regularization parameter updating method by control the reconstruction error residuals to obey a certain Gaussian distribution.

3.1 Noise Confidence Region Estimation

Note that the L2-norm term in (10) is under the assumption that the additive noise n_s is zero mean white Gaussian [9]. If $\hat{g}_i$ denotes the reconstruction result at ith iteration, then the reconstruction error residual $\Delta r = \mathrm{s}_s - \mathbf{A}\hat{g}$ at the end of ith iteration, ideally, should obey a white Gaussian distribution. Assume we choose an inappropriate λ that make the reconstruction result remove not only the noise but also parts of noiseless radar signal, then Δr will contain information that make its samples lager than white Gaussian noise. Based on this idea, we use a quantitative measure that verifies the similarity between the distribution of Δr and that of the noise.

Consider an additive noise random variable n with zero mean and finite variance σ. For any scalar value z, define a signature function $g(z, n)$:

$$g(z,n) = \frac{1}{m}\sum_{j=1}^{m} g\left(z, n_j\right), \quad g\left(z, n_j\right) = \begin{cases} 1 & |n_j| \le z \\ 0 & |n_j| > z \end{cases} \tag{11}$$

where m is the length of noise n. $g(z, n)$ is equivalent to sorting the absolute value of the noise elements n_j. In this case, the mean and variance of $g(z, n)$ can be expressed as:

$$\begin{aligned} E\left(g\left(z, n_j\right)\right) &= F(z) \\ Var\left(g\left(z, n_j\right)\right) &= \frac{1}{m}F(z)(1 - F(z)) \end{aligned} \tag{12}$$

where $F(z) = 2\phi(z/\sigma) - 1$ is the cumulative distribution function (CDF) of absolute value of n, $\phi(.)$ represents the CDF of Gaussian distribution. The NCR is a proper confidence region around the noise signature. Due to the noise signature structure, the

region is smaller than the corresponding confidence regions of the distribution of the additive noise itself. Since the additive noise n_s in radar system is zero mean white Gaussian noise, for each z and a high confidence probability p, the upper boundary $H(z)$ and lower boundary $L(z)$ of NCR can be derived using the Central Limit Theorem [10]:

$$\begin{aligned} H(z) &= F(z) + \delta\sqrt{\frac{1}{m}F(z)(1-F(z))} \\ L(z) &= F(z) - \delta\sqrt{\frac{1}{m}F(z)(1-F(z))} \end{aligned} \tag{13}$$

where δ is a positive number that makes the probability p close to 1. In this case, if $g(z, n_j)$ is between the upper and lower boundary, it means that n_j has a Gaussian like structure.

3.2 Regularization Parameter Updating

Figure 2 shows the NCR of residual Δr, under confidence probability p = 0.999 and noise variance $\sigma = 0.9409$ (we add white Gaussian noise so that the SNR of radar system is 0 dB). It can be seen that the upper boundary and lower boundary have divided the $(z, g(z, n))$ space into three regions where the NCR in the middle. At the end of each iteration, we calculated $g(z, \Delta r_j)$ and see whether $g(z, \Delta r_j)$ falls into NCR. If $g(z, \Delta r_j)$ falls into the region below NCR, it means that λ is too big that the regularization term in (10) has removed not only the noise but also parts of noiseless

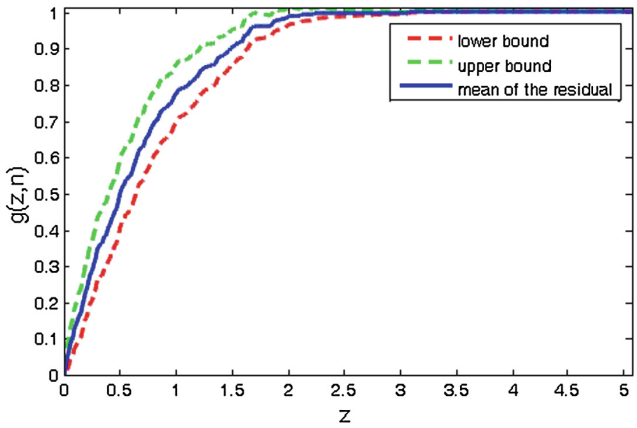

Fig. 2. NSR of the residual Δr, the upper bound and the lower bound are under confidence probability p = 0.999 with noise variance $\sigma = 0.9409$.

radar signal. If $g(z, \Delta r_j)$ falls into the region upon NCR, it means that λ is too small that only a part of noises are removed.

Here we proposed a simple regularization parameter updating method that force λ to moves toward NCR. We set a positive number $\alpha > 1$ and define λ_{j+1} as the regularization parameter in the next iteration:

$$\lambda_{j+1} = \begin{cases} \alpha \cdot \lambda_j & g(z, \Delta r_j) \in \text{region upon NCR} \\ \lambda_j / \alpha & g(z, \Delta r_j) \in \text{region below NCR} \end{cases} \tag{14}$$

If $g(z, \Delta r_j)$ falls into NCR, it means that the residual has a Gaussian like structure and the updating algorithm stops.

4 Experiments

In this section, we demonstrate the validity of the proposed method. We first conduct a simulation using single point scatterer to compare the reconstruction result. Table 1 lists the primary SAR parameters. Figure 3 shows the reconstruction results using Lq (q = 1/2) regularization optimization under different regularization parameters. These parameters are automatically chosen by our proposed method, start with $\lambda = 0.001$ and end with $\lambda = 0.1438$. We calculate the peak-to-sidelobe ratio (PSR) of different reconstruction results. It can be seen that the PSR increases monotonically with the update of λ, and the update stops when PSR is inf. The reconstruction result using the updated λ shows the absence of sidelobes as well as higher resolution than the result using initial λ. Figure 4 shows the reconstruction results using Lq (q = 2/3) regularization optimization, which get the same results.

Table 1. Parameters of SAR system and geometry.

Parameter	Simulation	RADARSAT-1
Slant range of radar center	50 km	1016.7 km
Radar center frequency	5000 MHz	5300 MHz
Platform velocity	110 m/s	7062 m/s
Pulse repetition frequency	175 Hz	1256.98 Hz
Pulse duration	2 μs	41.75 μs
Sampling rate	100 MHz	32.317 MHz

Next we test the validity of the proposed method on real SAR data from RADARSAT-1 in the fine mode-2 about Vancouver region. We applied our method to reconstruct the region of English Bay, where 6 vessels are sparsely distributed. The main radar parameters are shown in Table 1. Figure 5 shows the reconstruction results,

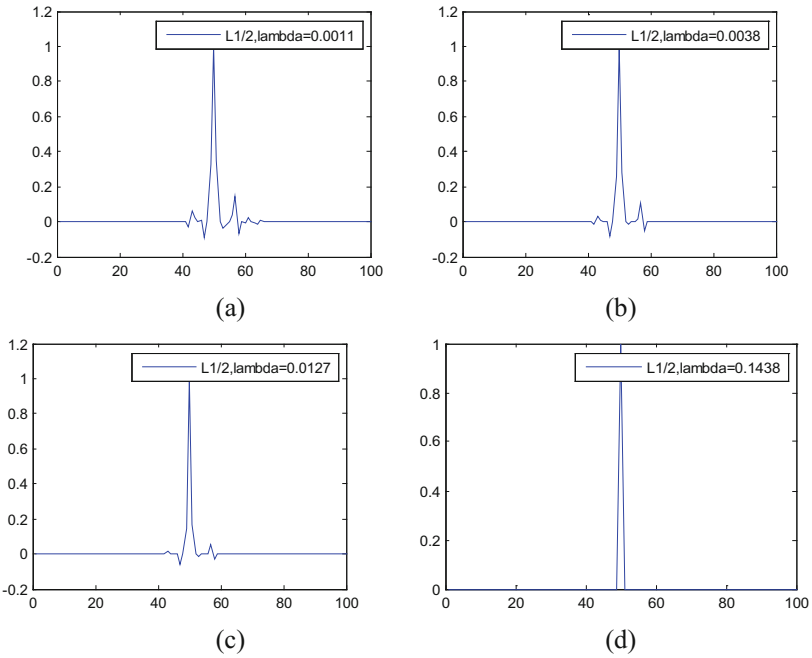

Fig. 3. Reconstruction results of a single point scatterer using Lq (q = 1/2) regularization optimization with different regularization parameters. (a) Imaging result with $\lambda = 0.0011$, PSR = 10.65 dB; (b) imaging result with $\lambda = 0.0038$, PSR = 11.55 dB; (c) imaging result with $\lambda = 0.0127$, PSR = 14.55 dB; (d) imaging result with $\lambda = 0.1438$, PSR = inf dB;

where the traditional SAR imaging result via Range Doppler Algorithm (RDA) under full sampling rate is shown in Fig. 5(a). Figure 5(b) shows the reconstructed result using L(1/2) regularization under $\lambda = 0.0038$ with 12.5% sampling rate than the Nyquist rate. Figure 5(c) shows the reconstructed result using L(1/2) regularization under the updated $\lambda = 0.01438$ with 12.5% sampling rate using the proposed method. Figure 6 shows the zoom in results of two vessels (in red boxes) in Fig. 5. It can be seen from Figs. 5 and 6 that the proposed method reconstructs higher quality images with reduced sidelobes at much lower sampling rate than traditional SAR imaging method and Lq regularization optimization method with fixed parameter.

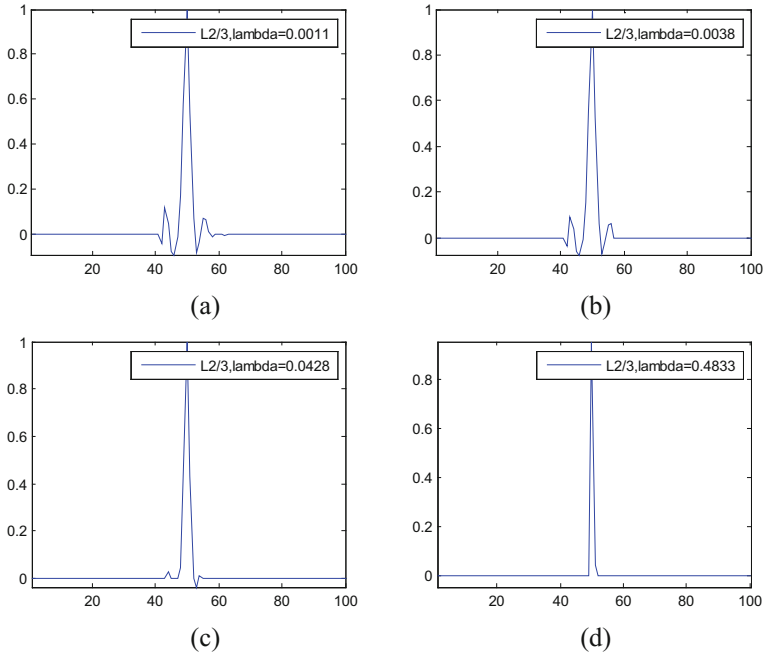

Fig. 4. Reconstruction results of a single point scatterer using Lq (q = 2/3) regularization optimization with different regularization parameters. (a) Imaging result with $\lambda = 0.0011$, PSR = 9.74 dB; (b) imaging result with $\lambda = 0.0011$, PSR = 10.32 dB; (c) imaging result with $\lambda = 0.0428$, PSR = 15.52 dB; (d) imaging result with $\lambda = 0.4833$, PSR = inf dB;

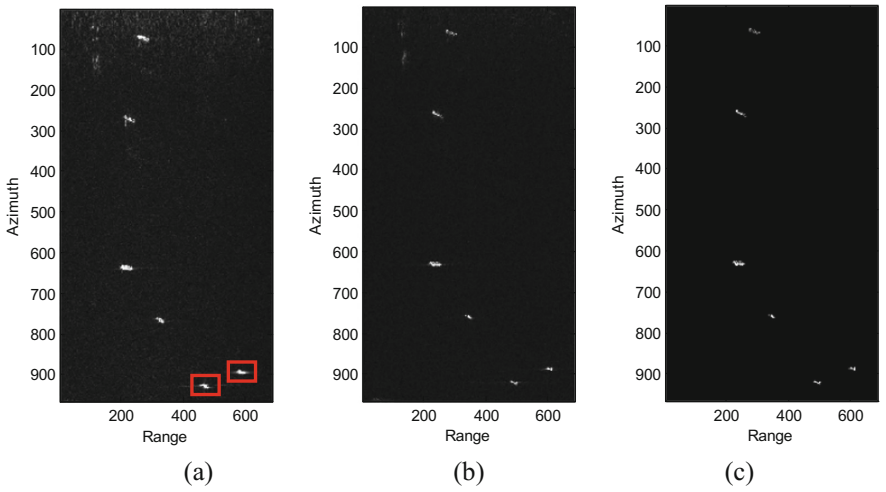

Fig. 5. Reconstructed results of RADARSAT-1 data. (a) The traditional radar image under the full sampling data, (b) reconstructed result using L(1/2) regularization under $\lambda = 0.0038$, (c) reconstructed result using L(1/2) regularization under $\lambda = 0.1438$. (Color figure online)

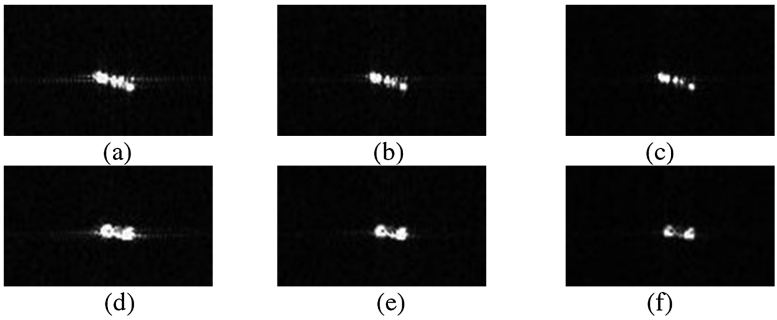

Fig. 6. Zoom in results of two vessels (in red boxes) in Fig. 5. (a) The traditional radar image under the full sampling data, (b) reconstructed result using L(1/2) regularization under $\lambda = 0.0038$, (c) reconstructed result using L(1/2) regularization under $\lambda = 0.1438$. (d)–(f) imaging results of another vessel.

5 Conclusion

In this paper, we present a regularization parameter determination method based on the properties of the additive noise. The proposed method is denoted by the noise confidence region (NCR), and validates the statistical properties of the error residuals. At the end of each iteration, the method categorizes the reconstruction result as well denoised, partially denoised, and over-smoothed. The method then updates the parameters so that the result falls into the well denoised region. The experiment results verify the validity of the new method.

References

1. Zeng, J., Fang, J., Xu, Z.: Sparse SAR imaging based on L1/2 regularization. Sci. China Inf. Sci. **55**, 1755–1775 (2012)
2. Logan, C.L.: An estimation-theoretic technique for motion-compensated synthetic-aperture array imaging. Ph.D. dissertation, Massachusetts Institute of Technology, Cambridge (2000)
3. Donoho, D.L.: Compressed sensing. IEEE Trans. Inf. Theory **30**(4), 1289–1306 (2006)
4. Candes, E., Romberg, J., Tao, T.: Robust uncertainty principles: exact signal reconstruction from highly incomplete frequency information. IEEE Trans. Inf. Theory **52**, 489–509 (2006)
5. Xu, Z.B., Zhang, H., Wang, Y., et al.: L1/2 regularizer. Sci. China Inf. Sci. **53**, 1159–1169 (2010)
6. Hashemi, S., Beheshti, S., Cobbold, S.C., et al.: Adaptive updating of regularization parameters. Sig. Process **113**, 228–233 (2015)
7. Vainikko, G.M.: The discrepancy principle for a class of regularization methods. USSR Comput. Math. Math. Phys. **22**(3), 1–19 (1982)
8. Hansen, P.: Analysis of discrete ill-posed problems by means of the L-curve. SIAM Rev. **34** (4), 561–580 (1992)
9. Samadi, S., Çetin, M., Masnadi-Shirazi, M.A.: Sparse representation based SAR imaging. IET Radar Sonar Navig. **5**(2), 182–193 (2011)
10. Beheshti, S., Hashemi, M., Zhang, X., Nikvand, N.: Noise invalidation denoising. IEEE Trans. Sig. Process. **58**(12), 6007–6016 (2010)